Geomicrobiology Journal
Publication details, including instructions for authors and subscription information:
http://www.tandfonline.com/loi/ugmb20

Bioleaching of Lizardite by Magnesium- and Nickel-Resistant Fungal Isolate from Serpentinite Soils—Implication for Carbon Capture and Storage

Zibo Li[a], Jie Xu[bc], H. Henry Teng[ab], Lianwen Liu[a], Jun Chen[a], Yang Chen[a], Liang Zhao[a] & Junfeng Ji[a]

[a] Key Laboratory of Surficial Geochemistry, Ministry of Education, School of Earth Sciences and EngineeringNanjing University, Nanjing, PR China

[b] Department of Chemistry, George Washington University, Washington, DC, USA

[c] Department of Geosciences, Virginia Tech, Blacksburg, Virginia, USA

Accepted author version posted online: 23 Oct 2013.Published online: 10 Dec 2014.

To cite this article: Zibo Li, Jie Xu, H. Henry Teng, Lianwen Liu, Jun Chen, Yang Chen, Liang Zhao & Junfeng Ji (2015) Bioleaching of Lizardite by Magnesium- and Nickel-Resistant Fungal Isolate from Serpentinite Soils—Implication for Carbon Capture and Storage, Geomicrobiology Journal, 32:2, 181-192, DOI: 10.1080/01490451.2013.835888

To link to this article: http://dx.doi.org/10.1080/01490451.2013.835888

Geomicrobiology Journal (2015) **32**, 181–192

ISSN: 0149-0451 print / 1521-0529 online
DOI: 10.1080/01490451.2013.835888

Taylor & Francis
Taylor & Francis Group

Bioleaching of Lizardite by Magnesium- and Nickel-Resistant Fungal Isolate from Serpentinite Soils—Implication for Carbon Capture and Storage

ZIBO LI[1], JIE XU[2,3], H. HENRY TENG[1,2], LIANWEN LIU[1]*, JUN CHEN[1], YANG CHEN[1], LIANG ZHAO[1], and JUNFENG JI[1]

[1]*Key Laboratory of Surficial Geochemistry, Ministry of Education, School of Earth Sciences and Engineering, Nanjing University, Nanjing, PR China*
[2]*Department of Chemistry, George Washington University, Washington, DC, USA*
[3]*Department of Geosciences, Virginia Tech, Blacksburg, Virginia, USA*

Received October 2012, Accepted August 2013

The major goal of this study was to evaluate the potential of fungal species indigenous to mine tailing soils in accelerating Mg release from lizardite (a polymorph of serpentine) at ambient T/P conditions. We characterized the culturable fungal isolates at three sampling sites representative of different degrees of mineral weathering by isolating the genomic subunits and internal transcribed spacer (ITS) rRNA genes using PCR and sequencing of cloned fragments. We chose the specific strain primarily identified as *Talaromyces sp.* for the further experiments with lizardite because of this strain's remarkable tolerance to high $[Mg^{2+}]$ (1 mol·L^{-1}) and $[Ni^{2+}]$ (10 mM·L^{-1}) levels in the screening test and its ubiquity in the most severely weathered samples. Results of dissolution experiments revealed that both magnesium-release rate and efficiency were significantly increased (e.g., by a factor of up to 15) in the presence of fungal cells than those in the abiotic controls. The enhanced dissolution of lizardite was mainly attributed to the fungal production of organic acids including oxalic acid, gluconic acid, formic acid, and fumaric acid added to the solution. The proton-promoted dissolution, however, was indicated not to be the only mechanism for fungus-lizardite interactions as much lesser Mg (in wt.%) was recovered in the abiotic system where the solution pH was constantly adjusted to match that of the fungal system. We also explored the dependence of fungal dissolution (of lizardite) on temperature and mineral particle sizes. In particular, we found that up to ~ 50 wt.% of Mg was released from mineral particles of ~ 50 μm within 30 days at 38°C, ~ 26% and 8% higher than that at 18°C and 28°C, respectively. At the same temperature of 28°C, the Mg-release efficiency increased from 12.2 wt% for particles of ~ 270 μm to 38.4 wt% for those of ~100 μm although no apparent difference was recognized when the particle size decreased below 100 μm. The nonlinear correlation of dissolution rates with particle surface areas suggested that the dissolution process was controlled by mineral surface-structural modification along with Mg release and by fungal cells' interaction with these surface structures. An amorphous layer of Mg-depleted silica was detected at the reacted mineral surface by scanning electron microscopy (SEM) and Fourier transform infrared spectroscopy (FTIR). Formation of glushinskite ($MgC_2O_4 \cdot 2H_2O$) was also observed when oxalate was accumulated to certain concentrations in the solution. Overall, this study showed that the isolated *Talaromyces sp.* was a promising bioagent to improve the efficacy of cation release from serpentine minerals for the purpose of carbon sequestration and resource recovery.

Keywords: fungal bioleaching, lizardite, magnesium release, mineral carbonation, *Talaromyces sp.*

Introduction

Anthropogenic CO_2 emission over the past hundred years has been linked with global-wide environmental changes. As such, fundamental research aiming at curtailing CO_2 buildup has become crucial for the sustainability of the human society (Pacala and Socolow 2004). Amongst the strategies proposed for CO_2 capture and storage (CCS), mineral carbonation is one alternative that mimics natural weathering of ultramafic rocks by converting CO_2 gas into solid carbonate minerals through (aqueous) reactions with divalent cations (e.g., Ca^{2+} and Mg^{2+}). To date, a range of substrate materials including oxyhydroxides, silicate, and industrial slags are being tested for their potential in mineral carbonation (Béarat et al. 2002; Goff and Lackner 1998; Huijgen et al. 2005; Stolaroff et al. 2005).

Serpentine may be a suitable raw material for mineral carbonation because of its high magnesium content (~ 40% of MgO) and large quantities in nature. Although carbonation of serpentine is a thermodynamically favorable process (Herzog

*Address correspondence to Lianwen Liu, Key Laboratory of Surficial Geochemistry, Ministry of Education, School of Earth Sciences and Engineering, Nanjing University, Nanjing 210093, PR China; Email: liulw@nju.edu.cn

2002), which can be described as the following equation:

$$Mg_3Si_2O_5(OH)_4 + 3CO_2 \rightarrow 3M_gCO_3 + 2SiO_2 + 2H_2O \quad \Delta G_f^0 = +64 \text{ kJ/mole} \quad (1)$$

the overall kinetics for Equation 1 is rather slow, mainly limited by the magnesium-release rate. In previous studies, different P/T conditions have been tested and various chemicals such as mineral acids (Lackner et al. 1995; Teir et al. 2007a, 2007b, 2009), organic acids (Teir et al. 2007b) and organic salts (Krevor and Lackner 2011) have been used to optimize the carbonation process via enhancing the magnesium extraction. Most of these processes, however, are unfeasibly costly due to high material and energy consumptions, and thus, are difficult to scale up into industrial levels.

Compared to the numerous investigations on abiotic serpentine dissolution, biologically mediated dissolution processes have yet to be fully appreciated. Nonetheless, a volume of studies has confirmed the potential of microorganisms in releasing magnesium from ultramafic rocks. Some of these studies were focused on bacteria capable of sulfur oxidation and sulfuric acid production. For example, a recent one evaluated the effect of *Acidithiobacillus spp.* on bioleaching of ultramafic tailings and identified an apparent increase in the Mg^{2+} extraction rate in the presence of bacterial cells (Power et al. 2010). Meanwhile, fungi and fungal symbionts have also been recognized for their enhancing roles in rock weathering and mineral dissolution (Banfield et al. 1999; Burford et al. 2003a, 2003b; Favero-Longo et al. 2007; Gadd and Raven 2010). As early as 1970, Jackson and Keller (1970) observed that lichen-covered basalt released magnesium 1–2 orders of magnitude faster than the bare ones at ambient conditions. And a more recent study (Daghino et al. 2009) showed that up to 22.3 wt.% of magnesium could be recovered from chrysotile by *Verticillium Ieptobactrum* within 20 days, ∼ twice as much as that in abotic media.

Fungi are eukaryotic organisms that constitute the dominant biomass in a variety of environments. The ubiquity of fungi in nature is closely related to their explorative growth habit, physiological adaptation and flexibility, and resistance to extreme environmental conditions, such as metal toxicity, irradiation, and desiccation (Gadd 2007; Gleeson et al. 2005; Gorbushina 2006; Gulis et al. 2006). Several studies (Adeyemi and Gadd 2005; Burford et al. 2003a; Castro et al. 2000; Fomina et al. 2010; Gadd and Raven 2010) indicated that fungi were more effective in silicate weathering than bacteria or archaea. And this ascendancy was probably attributed to two factors: (a) fungi produce more effective organic acids than bacteria (Palmer et al. 1991); and (b) fungal hyphae are more likely to access mineral (sub)surfaces to exert physical forces (Favero-Longo et al. 2007; Hoffland et al. 2004).

To further explore the fungus-serpentine interactions, we examined the fungal isolates indigenous to serpentinite soils in Donghai, China and evaluated the fungal effect on serpentine dissolution systematically. The major objective of this study was to isolate a potent strain that may accelerate and maximize Mg^{2+} release from high-Mg minerals (i.e., lizardite) for the purpose of CCS. We also probed into the fungus-mediated dissolution mechanisms by analyzing the major components of fungal metabolites and evaluating the effects of temperature and particle size on Mg^{2+} release rates and efficiency. The specific strain chosen for the dissolution experiments showed remarkable tolerance to high concentrations of Mg^{2+} and Ni^{2+}, and enhanced the Mg^{2+} release efficiency up to ∼ 50 wt.% at ambient conditions.

Materials and Methods

Sampling Site

The serpentinite soils for fungal isolation were obtained from a site in Donghai, China (34°37′ N, 118°30′ E), which lies on top of massive serpentinite occurring from metamorphism of Proterozoic ultramafic rocks. We collected three samples, labeled as 3-4R, 3-6R, and 3-9R, respectively, from different depths of the soil profile using sterile spatulas. These samples were then maintained in sterile plastic containers at 4°C for a few hours before being used for fungal isolation. The extent of weathering for the samples was found to inversely correlate with their depths in the profile, among which 3-4R was most similar to the parent rock in chemical compositions and contained the highest wt.% of magnesium (∼23%) whereas 3-9R was most severely weathered and contained the least wt.% of magnesium (∼9%). The major mineral components were identified as lizardite and a small amount of clinochlore by X-ray diffraction (XRD) for all three samples while a fraction of quartz, nimite, nontronite and calcite was detected only in 3-6R and 3-9R.

Analysis of the Culturable Fungi

For fungal isolation, 10 g of the soil sample (3-4R, 3-6R, or 3-9R) was added into 100 mL of sterilized DI water, shaken for 2 h at 50 rpm in a water bath set to 28°C. The suspension was then allowed 30 min in still mode for particles to settle. Aliquots of 200-μL supernatant were then spread and maintained at 28°C on malt agar plates (20 g·L^{-1} malt extract with 18 g·L^{-1} agar, Sinopharm, China), amended with antibiotics (40 mg·L^{-1} gentamycine, Amersco, USA; and 30 mg·L^{-1} streptomycin, Sigma Aldrich, USA). At least three replicates were prepared for each sample and for each suspension. Upon incubation for ∼ two weeks, developed fungal colonies were separated and further purified on fresh plates (with the same medium). The culturable fungi were identified by their morphological characters with dichotomous keys.

The sequencing of the Internal Transcribed Spacer (ITS) for the nuclear rDNA region was also carried out following polymerase chain reaction (PCR) amplification with the universal fungal primers ITS1F (CTTGGTCATTTAGAGGAAGTAA) and ITS4 (TCCTCCGCTTATTGATATGC). Specifically, we cultivated each isolate in the Czapek mineral medium ($NaNO_3$ 3 g·L^{-1}, K_2HPO4 1.72 g·L^{-1}, $MgSO4{\cdot}7H_2O$ 0.5 g·L^{-1}, KCl 0.5 g·L^{-1}, $FeSO4{\cdot}7H_2O$ 0.01 g·L^{-1}, and glucose 20 g·L^{-1}) at 28°C (120 rpm) for 7 days. Genomic DNA of the isolate was then extracted using the Biospin Fungus Genomic DNA Extraction Kit (Japan) following the protocol provided

by the manufacturer. To reduce the bias in DNA extraction, three separate extractions were carried out for each sample. The ITS region was amplified using ITS1F and ITS4 primers (Gardes and Bruns 1993). The PCR mixture contained 29 μL of deionized H_2O, 5 μL of buffer, 5 μL of $MgCl_2$, 5 μL of deoxyribose nucleotide, 1 μL of strain DNA template, 2 μL of each primer pair, and 1 μl of DNA polymerase. The PCR cycle was: 95°C for 5 minutes in the initial denaturation, followed by 34 cycles of 95°C for 30 sec, 54°C for 30 sec, and 72°C for 1 min, with a final extension of 72°C for 10 min. The PCR products were run on 1% low-melting-point agarose gels, and then excised from the gel and purified for sequencing. The sequences obtained were compared to the National Center for Biotechnology Information (NCBI) database using the BLAST algorithm.

Mg^{2+} and Ni^{2+} Screening of the Fungal Isolates

The fungal isolates were examined for their resistance to Mg^{2+} and Ni^{2+}, which may be indicative of the potential viability of fungal cells in the lizardite particle suspensions. Each type of the fungal isolates was incubated in a 250-mL Erlenmeyer flask containing 100 mL of Czapek mineral medium, supplemented with either 600 mM – 1 M of Mg^{2+} or 10 mM of Ni^{2+}. All screening experiments were performed in three replicates. The variation of fungal biomasses (± wt.%) in each case was evaluated after 10 days of incubation at 28°C and 120 rpm. The strain that managed to grow well in both 1M Mg^{2+} and 10 mM Ni^{2+} solutions was selected for the bioleaching experiments.

Preparation and Characterization of Lizardite Particles

The lizardite samples used in the experiments were obtained from the same source as the serpentinite soils. These samples contained ~38 wt.% of MgO and <5 wt.% of Fe_2O_3 based on chemical analyses, and XRD data confirmed lizardite as the major mineral component although a tiny amount of clinochlore was also found to be present. The mineral was crushed using a ball mill and serially sieved to separate particles of different size fractions. The size fraction in 250–325, 150–200, and 50–100 mesh (corresponding grain size 45–50 μm, ~100 μm, and >270 μm) were collected for experimental use. The specific surface area of the particles in the 250–325 mesh range was determined to be 25.5 m^2g^{-1} using the nitrogen BET adsorption method (ASAP 2020, Micromeritics, USA). The particles were oven dried at 50°C for 24 h prior to use.

Dissolution Experiments

Powdered lizardite of certain particle sizes was autoclaved at 121°C for 20 min before 0.5 g of particles were added to 100 mL of Czapek medium in 250-mL Erlenmeyer flasks. The fungal cells used for the dissolution experiments were harvested at their log phase by a 0.22-μm filter, rinsed three times in 0.8% saline water, and resuspended in fresh Czapek media. Aliquots of 1-mL cell culture solution were mixed with the lizardite-containing medium, following which the mixtures were maintained at 18, 28, and 38°C, respectively, in a shaking incubator (running at 120 rpm). Three types of controls were designed for the 28°C experiments to determine the various background effects. Controls A and B concerned the lizardite dissolution in sterile Czapek medium and DI water, respectively, whereas control C monitored fungal growth in the absence of lizardite in Czapek medium. To evaluate the acid effect on magnesium release rate and efficiency, the pH of control B was adjusted constantly to match that measured in the fungal system. Twelve replicates were prepared for each bioleaching or control experiment at the start.

The pHs of the experimental solutions were monitored regularly (on days 3, 7, 15, and 30). The Mg^{2+} and Si concentrations in each sample were also determined using inductively coupled plasma-optical emission spectroscopy (ICP-OES) (iCAP 6300, England). In specific, 10 mL of each solution was sampled and filtered through a 0.22-μm PVDF membrane, and then acidified to ~ pH 2 with 1% HNO_3 before being analyzed by ICP-OES. For each case, triplicate samples were examined and for each sample, triplicate measurements were performed.

Fungal consumption of glucose and production of organic acids were also quantified and compared between the different experimental systems (i.e., 18°C, 28°C, and 38°C). Glucose concentrations in the samples were measured using the Glucose Assay Kit II (Biovision, USA) and a microplate reader (Bio-TEK) with the absorbance wavelength set at 450 nm. A standard curve for the measurements was established using glucose solutions of 0, 0.04, 0.08, 0.12, 0.16 and 0.2 $nmol{\cdot}\mu L^{-1}$ respectively. The contents of organic acids produced by fungi were analyzed by an high-performance liquid chromatography (HPLC) (Agilent 1200, USA) equipped with Zorbax SB-C8 (4.6 × 250 mm, 5 micron) and XDB-C8 (4.6 × 75 mm, 3.5-μ) columns (sequentially installed) and a diode array detector (DAD), which has a detection limit of ~ 3.2 $\mu mol{\cdot}L^{-1}$.

The flow rate was set to 0.7 $mL{\cdot}min^{-1}$ to ensure effective separation of different types of organic acids. We used 50 mM KH_2PO_4 as the mobile phase and adjusted the initial pH of sample solutions to ~2.5 using H_3PO_4. For analysis of gluconic acids, we employed a different SB column (4.6 × 250 mm, 5 μ), and used different mobile phase (0.1% H_3PO_4) as well as flow rate (1.0 $mL{\cdot}min^{-1}$). The reference reagents used in the analyses including oxalic acid anhydrate, citric acid (>99.5%), acetic acid (>99.7%), D-gluconic acid sodium, fumaric acid, L-(+)-tartaric acid, formic acid, and L-(-)-malic acid (>99.5%), were of HPLC grade and purchased from Sigma-Aldrich (USA).

Surface-Structure Analysis of Reacted Minerals

The mineral-hyphae aggregates were collected by filtration (GC-SM filters, Whatman), and rinsed with assistance of sonication in pure alcohol for 10 min. A small drop of mineral suspension was then placed on a glass slide and air-dried for analysis by scanning electron microscopy (SEM) coupled with energy-dispersive spectroscopy (EDS). The reacted minerals in the dissolution experiment at 28°C were also analyzed by

Table 1. Culturable fungal isolates in the serpentinite soil samples 3-4R, 3-6R, and 3-9R, respectively, from Donghai, China

Sample	Fungal isolations	Sample	Fungal isolations	Sample	Fungal isolations
3-4R	*Penicillium sp. (1)*	3-6R	*Penicillium sp. (1)*	3-9R	*Penicillium sp. (3)*
	Penicillium citrinum (1)		*Penicillium citrinum (2)*		*Penicillium citrinum (1)*
	Penicillium simplicissimum (1)		*Penicillium simplicissimum (1)*		
	Penicillium diversum (4)				
			Penicillium citreonigrum (1)		*Penicillium citreonigrum (2)*
			Botryotinia fuckeliana (1)		*Botryotinia fuckeliana (1)*
			Talaromyces flavus (1)		*Talaromyces flavus (2)*
			Paecilomyces marquandii (1)		*Paecilomyces tenuis (1)*
			Trichoderma asperellum (7)		*Penicillium pinophilum (1)*
			Cosmospora consors (1)		*Penicillium janthinellum (1)*
			Fusarium oxysporum (1)		*Cladosporium cladosporioides (1)*
			Microdochium nivale (1)		*Alternaria alternata (2)*
			Monascus purpureus (1)		

Note: The naming of the fungal isolates was based on BLAST analyses using the NCBI database and primary phylogenetic analyses using the neighbor-joining method. The number in the bracket refers the number of fungal species isolated from the specific soil. The list of species for each sample is not given in any particular order.

Fourier transform infrared spectroscopy (FT-IR) to characterize the transformation of surface bond structures. For each dissolution experiment, we monitored the mineral phases present in the samples at the beginning and end of the experiment using XRD analyses.

Results

Culturable Fungi in the Soil Profile and Their Metal-Resistance

A total of 30 fungal species were isolated from the serpentinite soils collected in Donghai, China (Table 1). These isolated species belonged to a range of common genera including *Penicillium* (13), *Talaromyces* (3), *Trichoderma* (3), *Paecilomyces* (2), *Botryotinia* (2), *Fusarium* (1), *Cladosporium* (1), *Alternaria* (1), *Clavicipitaceae, Cosmospora* (1), *Microdochium* (1), *Monascus* (1), and *Plectosphaerella* (1). The number of culturable fungal isolates showed a positive correlation with the weathering extent of the soil samples. For example, in the least weathered sample (3-4R), only species within the *Penicillium* genus were identified; in comparison, more "diverse communities" were found in the 3-6R and 3-9R samples based on the number of different sequences isolated.

The results of screening tests showed that, ∼40% of the fungal isolates could survive in 1 M Mg^{2+}-amended growth medium, and ∼23% of the isolates could survive in 10 mM Ni^{2+}-amended medium. Details of the screening results were shown in Table 2. We compared the initial and end biomasses in the metal-amended medium (M^0_{metal}, M^e_{metal}) with those in the metal-free medium (M^0_{free}, M^e_{free}), and defined the growth condition as "robust growth" when $\left(M^{end}_{metal} - M^0_{metal}\right) > 0$ and $\left(\frac{M^{end}_{metal} - M^0_{metal}}{M^{end}_{free} - M^0_{free}}\right) \times 100\% > 90\%$ or "suppressed growth" when $\left(M^{end}_{metal} - M^0_{metal}\right) > 0$ but $\left(\frac{M^{end}_{metal} - M^0_{metal}}{M^{end}_{free} - M^0_{free}}\right) \times 100\% < 50\%$. If $\left(M^{end}_{metal} - M^0_{metal}\right) \leq 0$, then the condition was defined as "no growth." Among the isolates, only the one primarily identified as *Talaromyces sp.* based on its colony characteristics and genomic sequences, was found to grow well in the presence of 1 M Mg^{2+} or 10 mM Ni^{+}. This species was also prolific in acid production and achieved the highest Mg^{2+}-release efficacy in our pretrials. Thus, the *Talaromyces sp.* was chosen for the following dissolution experiments.

Mg-release efficiency

Abiotic vs. Biotic

The Mg-release efficiency (in wt.%) in the absence and presence of fungal cells at 28°C showed apparent difference from each other (Figure 1). For the abiotic controls, ∼8.9 wt.% of Mg was released from lizardite in the noninoculated Czapek medium over 30 days of experiment and ∼3.0 wt.% of Mg was released in the pH-adjusted DI water. By contrast, up to 40 wt.% of Mg was released in the fungal system, ∼5–10 times higher than that in the controls. The formation of plateaus was observed around days 10–15 in the dissolution curves (both biotic and abiotic), indicating that these experimental systems reached equilibrium around days 10–15.

Effect of Temperature and Particle Sizes

Fungal bioleaching of lizardite (in terms of Mg-release rates and efficiency) showed a strong dependence on temperature and particle sizes (Figure 2 and Figure 3). In the temperature range of 18–38°C, the maximum Mg-release efficacy was achieved at 38°C, which was ∼ 47.9 wt.%; when the temperature was decreased to 28°C or 18°C, the efficiency was at a much lower level of ∼ 39.4 wt.% or 21.6 wt.% (Figure 2). The initial Mg-release rates (R) also showed a similar trend as $R_{38} > R_{28} > R_{18}$. It seemed that the 38°C and 28°C systems

Table 2. Growth conditions of each fungal isolate in the Mg^{2+} or Ni^{2+} supplemented medium for 10 days

Phenotype No.	Fungi isolations	Mg^{2+} 600 mM	Mg^{2+} 800 mM	Mg^{2+} 1 M	Ni^{2+} 10 mM
1	*Penicillium sp.*	++	++	+	×
2	*Penicillium janthinellum*	+	×	×	×
3	*Penicillium diversum*	++	++	++	+
4	*Penicillium citreonigrum*	+	×	×	+
5	*Trichoderma asperellum*	+	+	+	×
6	*Penicillium sp.*	+	×	×	×
7	*Trichoderma asperellum*	++	++	++	+
8	*Trichoderma asperellum*	++	++	++	×
9	*Paecilomyces tenuis*	++	++	+	++
10	*Penicillium pinophilum*	++	+	+	+
11	*Penicillium citreonigrum*	+	+	+	+
12	*Penicillium sp.*	+	×	×	+
13	*Cosmospora consors*	++	++	++	+
14	*Penicillium citrinum*	+	+	×	×
15	*Botryotinia fuckeliana*	+	×	×	×
16	*Penicillium simplicissimum*	+	×	×	+
17	*Penicillium diversum*	+	+	+	++
18	*Cladosporium cladosporioides*	++	++	+	+
19	*Talaromyces flavus*	++	++	++	++
20	*Paecilomyces marquandii*	++	++	+	++
21	*Fusarium oxysporum*	++	++	++	+
22	*Alternaria alternate*	+	×	×	×
23	*Penicillium citrinum*	+	+	+	×
24	*Penicillium citrinum*	++	++	++	+
25	*Microdochium nivale*	++	++	++	+
26	*Talaromyces flavus*	++	++	++	++
27	*Talaromyces flavus*	++	++	++	++
28	*Botryotinia fuckeliana*	++	++	++	×
29	*Monascus purpureus*	++	++	+	++
30	*Plectosphaerella cucumerina*	++	++	++	×

++ Robust growth; + Suppressed growth; × No growth

Note: we compared the initial and end biomasses in the metal-amended medium (M^0_{metal}, M^e_{metal}) with those in the metal-free medium (M^0_{free}, M^e_{free}). If $\left(M^{end}_{metal} - M^0_{metal}\right) > 0$ and $\left(\frac{M^{end}_{metal} - M^0_{metal}}{M^{end}_{free} - M^0_{free}}\right) \times 100\% > 90\%$, the growth condition was defined as "robust; if $\left(M^{end}_{metal} - M^0_{metal}\right) > 0$ and $\left(\frac{M^{end}_{metal} - M^0_{metal}}{M^{end}_{free} - M^0_{free}}\right) \times 100\% < 50\%$, the condition was defined as "suppressed": If $\left(M^{end}_{metal} - M^0_{metal}\right) \leq 0$, then the condition was defined as "no growth."
The name for each isolated was assigned based on BLAST analysis using the NCBI database and primary phylogenetic analysis using the neighbor-joining method.

reached equilibrium at ~ day 10 and day 15, respectively, while the 18°C system did not reach equilibrium until the end of the experiment (day 30).

The Mg-release efficiency for lizardite particles of different size fractions at 28°C was also examined (Figure 3). For particles above 270 μm, only 12.2 wt.% of Mg was released after 30 days; in comparison, 38.4 wt.% of Mg was released after the same duration for particles of ~100 μm. When the particle size dropped to ~50 μm, however, the efficiency was not further increased (~39.4 wt%). Due to the detection limit of the B.E.T. method, we did not manage to measure the surface areas of the larger particles (i.e., those ~100 μm and >270 μm) accurately. Yet it was recognizable that both the initial Mg-release rate and the ultimate Mg-release efficiency showed nonlinear relationships with the available particle surface areas.

Fungal Production of Organic Acids

We found that at 28°C, the solution pH increased steadily over time in the absence of fungal cells, due to the discharge of dissolved silica into the system, whereas in the presence of fungal cells, the solution pH dropped to ~4.6 (by almost one unit) within the first three days and was followed by a rebound to ~ 6 from day 4–day 30 (Figure 2). In the lizardite-free medium with fungal growth, the pH remained relatively constant for about 16 days after the initial decline to ~ 4.2, and then showed a slight increase at the end of the experiment. The pH variations in the abiotic and fungal systems under different temperatures were quite similar to each other.

High concentrations of organic acids and other biological metabolites were detected in the experimental solutions in the presence of fungal cells. We found that organic acids, including

Table 3. Measured pH and concentrations of major organic acids (μmol·L^{-1}) and glucose (g·L^{-1}) in the culture media after 7 days of fungal growth in the presence of lizardite (bioleaching) and absence of lizardite (Control C) at 18°C, 28°C, and 38°C

T (°C)	Exp.	pH	Oxalic acid#	Gluconic acid #	Tartaric acid #	Formic acid #	Malic acid #	Citric acid #	Acetic acid #	Fumaric acid #
18	Contact	4.67	316	12132	338	1428	<	<	<	<
	Control C	4.40	58	8770	240	965	<	43	124	<
28	Contact	4.96	21548	21636	174	18340	168	<	520	2089
	Control C	3.89	71	17545	396	1800	61	<	600	125
38	Contact	4.75	13779	46296	420	9958	440	87	3978	611
	Control C	4.38	252	26335	389	2321	153	33	844	533

Note: "<": below HPLC detection limit.

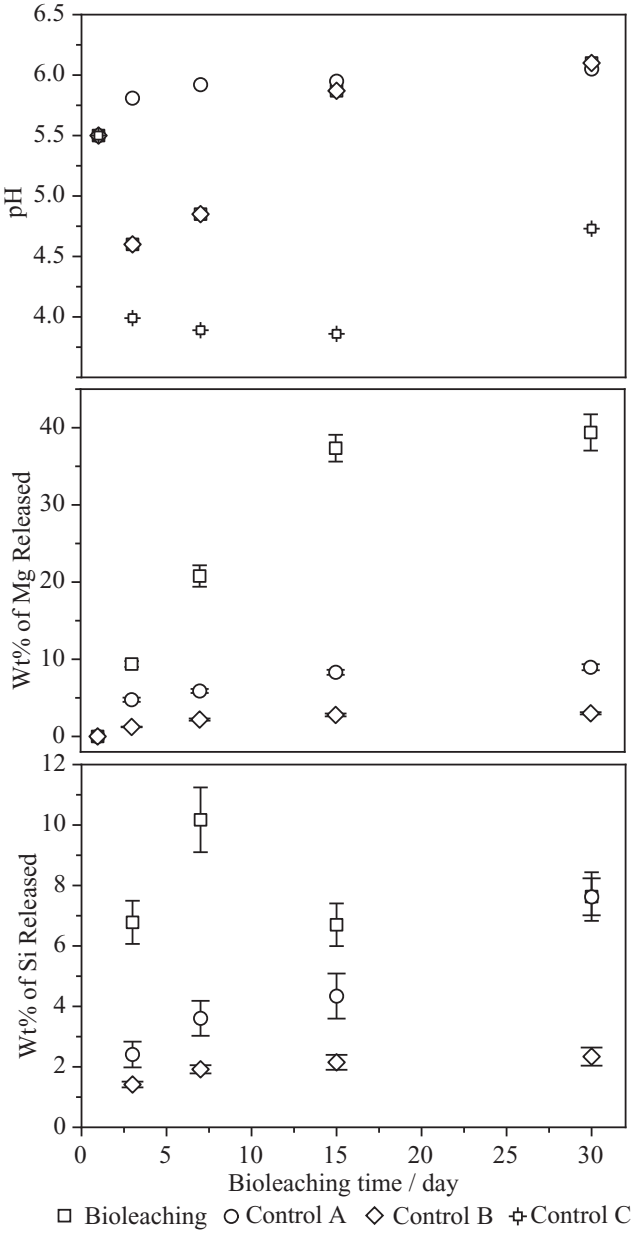

Fig. 1. pHs, weight percentage of Mg and Si (wt%) released from lizardite at 28°C.

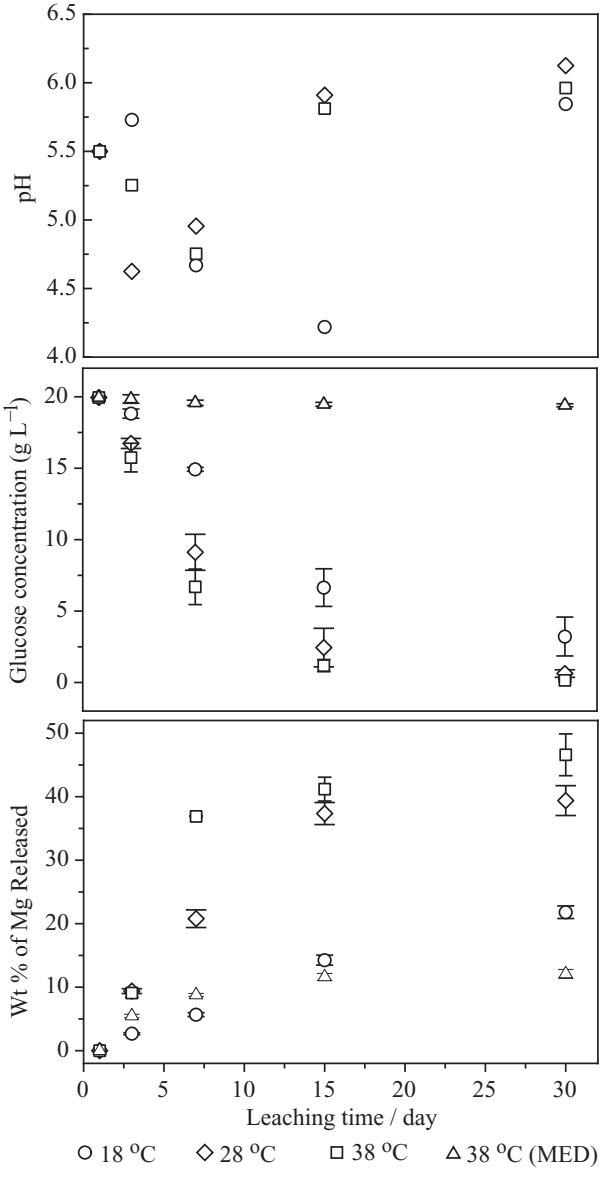

Fig. 2. pHs, glucose concentration (g·L^{-1}) and wt% of Mg released at 18, 28, and 38°C in the bioleaching experiments.

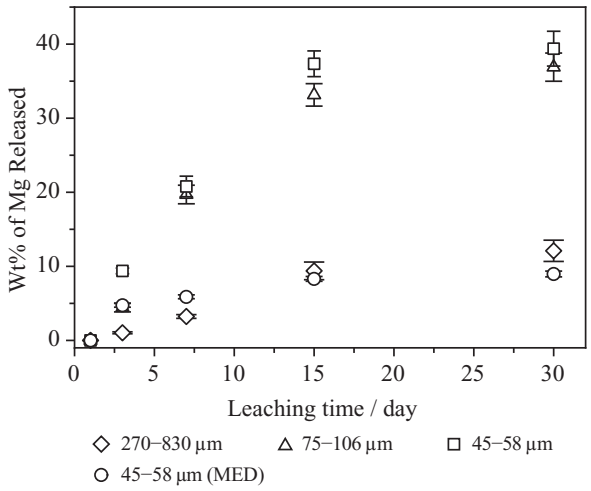

Fig. 3. Weight percentage of Mg (wt%) released from lizardite particles of three different size fractions, 270–830 μm, ~100 μm, and 45–50 μm, respectively, at 28°C.

oxalic acid, gluconic acid, tartaric acid, formic acid, malic acid, citric acid, acetic acid, and fumaric acid, were produced by fungal cells either with or without lizardite present in the system (Table 3).

The presence of mineral particles, however, seemed to have greatly enhanced the production of organic acids as 13,779 μmol·L^{-1} of oxalic acid and 3978 μmol·L^{-1} of acetic acid were excreted in the lizardite-positive medium compared to ~252 μmol·L^{-1} of oxalic acid and 844 μmol·L^{-1} of acetic acid in the lizardite-negative medium at the same temperature (28°C). It was also revealed that the temperature change might have a significant effect on fungal production of organic acids. In particular, at 38°C, 13,779 μmol·L^{-1} of oxalic acid, 46,296 μmol·L^{-1} of gluconic acid, 9958 μmol·L^{-1} of formic acid, and 3978 μmol·L^{-1} of acetic acid were determined in the bioleaching solution (lizardite+, fungus+), whereas much lower levels of correspondingly 316 μmol·L^{-1}, 12,132 μmol·L^{-1}, 1428 μmol·L^{-1}, and below detection limit were determined at 18°C. Moreover, malic, citric, and fumaric acids that were produced in the 38°C fungus-lizardite system were not detected in the 18°C system.

The initial glucose concentration in the culture medium was 19.96 g·L^{-1}. Analyses of glucose concentrations in the experimental solutions indicated that, no glucose was consumed in the noninoculated control (Control A) and the glucose consumption rates increased with increasing temperature. Specifically, 6.70 ± 1.24 g·L^{-1} of glucose remained in the 38°C fungus-lizardite system at day 7, while 9.12 ± 1.26 and 14.92 ± 0.14 g·L^{-1} remained in the 28°C and 18°C systems, respectively. At the end of the experiments (day 30), the glucose had almost been used up in the 38°C or 28°C solution, but 3.22 ± 1.36 g·L^{-1} remained in the 18°C solution. Interestingly, the fungal growth in the absence of lizardite (i.e., Control C) consumed much less glucose than that in a lizardite-positive environment, with 10.81 g·L^{-1}, 7.82 g·L^{-1}, and 5.77 g·L^{-1} available at day 30 for the 18°C, 28°C, and 38°C, respectively.

Surface Structures of Reacted Lizardite

The SEM micrographs coupled with EDS analysis revealed that, the pristine mineral surfaces were relatively smooth and had a Mg/Si ratio of 1.48 (close to the theoretical value of 1.5), whereas the fungus-reacted mineral surface became dramatically roughened and Mg-depleted (Figure 4). An amorphous layer of silica was detected on top of the reacted mineral surfaces. It was noticed that in the abiotic control (Control B) of similar pH as the fungal system, the Mg/Si ratio only decreased slightly to ~1.34.

The FT-IR spectra for the pristine and reacted minerals collected at days 3, 7, 15, and 30 showed clear transformation of the surface bond structures in the bioleaching process (Figure 5). The bend at 3702 cm^{-1} assigned to the in-phase outer Mg-OH stretch, was visible in the pristine mineral. As the bioleaching occurred, this bend shifted to lower wavenumbers of 3683–3689 cm^{-1} and decreased in intensity, which indicated that the in-phase outer Mg-OH stretch might have transformed into inner Mg-OH stretch (Kloprogge et al. 1999). The stretching bond of Si-O corresponding to the bend at 1155 cm^{-1} (Post and Borer 2000) also seemed to become significantly weaker over time, whereas a new bend appeared in the region of 796 cm^{-1} and started to increase in intensity on day 3.

Substantial amounts of rhombohedra-shaped crystals were observed at the surface of reacted minerals (Figure 6). These crystals had a size of 3–5 μm, and were identified as glushinskite ($MgC_2O_4{\cdot}2(H_2O)$) by EDS and XRD analyses.

Discussion

Fungal Isolates in Serpentine Environments

We compared the identified fungal isolates indigenous to the serpentinite soils (in Donghai, China) with those reported in previous studies, and found a spectrum of common species including *Penicillium*, *Trichoderma, Fusarium*, and *Cladosporium* (Daghino et al. 2008; Pal et al. 2006). Importantly, a positive correlation was recognized between the weathering extent of the soils (in terms of Mg-depletion) and the number of fungal isolate(s) in each serpentinite soil. Thus, the culturable fungi in this specific environment seemed to have played an undeniable role in weathering the magnesium silicate minerals.

The potential of different fungal species in weathering serpentine minerals, however, varied greatly in our pretests, indicating that only some specific strains might be effective bioagents to enhance the Mg release from ultramafic sediments and rocks. The isolate used in the present study (*Talaromyces* sp.) showed high tolerance to Mg^{2+} and Ni^{2+} and was a prolific producer of organic acids as well as other metabolites including polysaccharides and enzymes.

It has been proposed in previous studies that the organic acids excreted by fungi were influenced by multiple factors including the pH and buffering capability of the environment, the carbon, phosphorus, and nitrate sources, and the presence of certain metals (Dutton and Evans 1996; Fomina

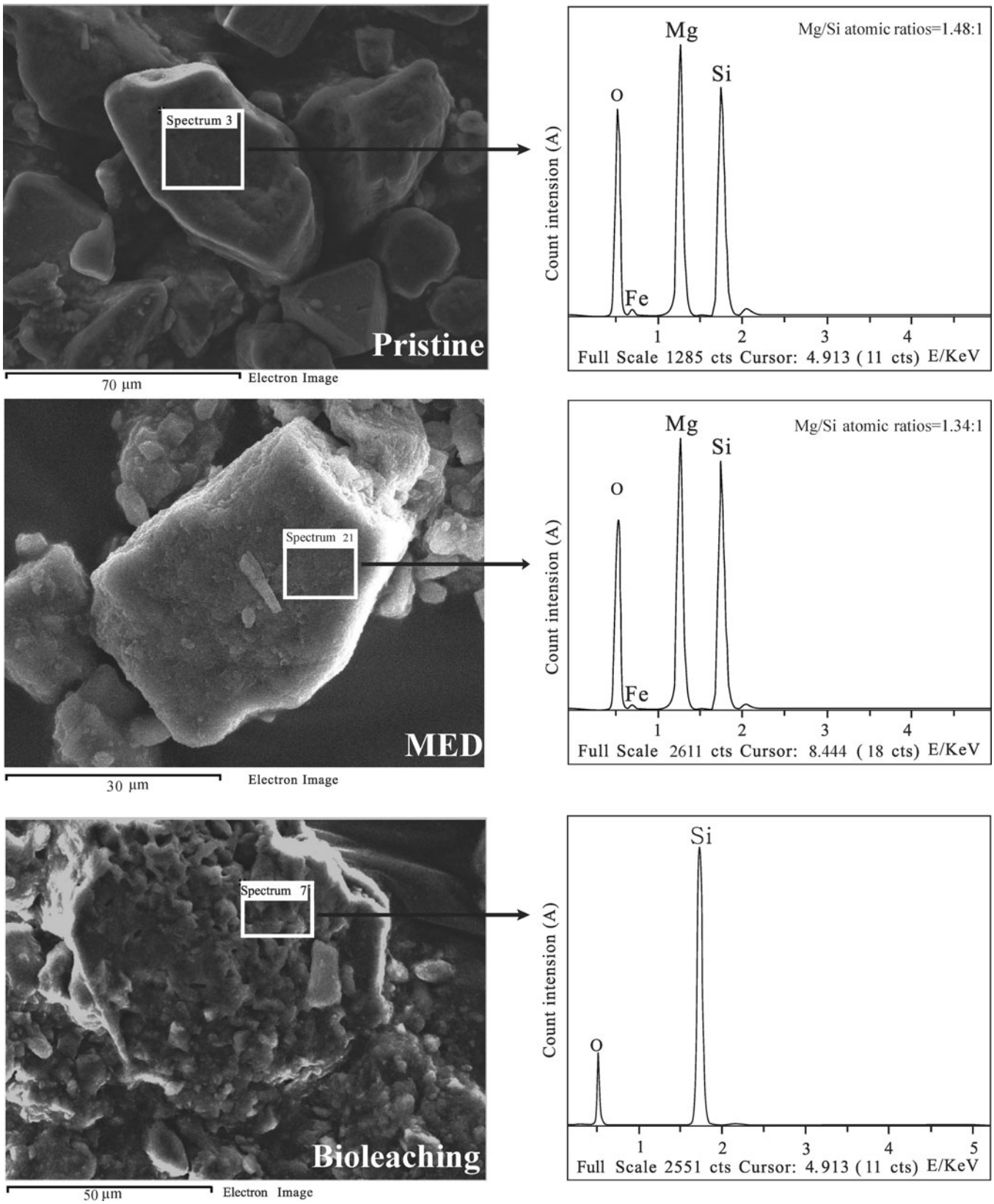

Fig. 4. Scanning electron microscopy micrographs of the pristine (upper left) and reacted lizardite in control B (middle left) or in bioleaching experiments (lower left). Corresponding EDS analyses (right) revealed that Mg was depleted at the surface of reacted minerals from the fungal system.

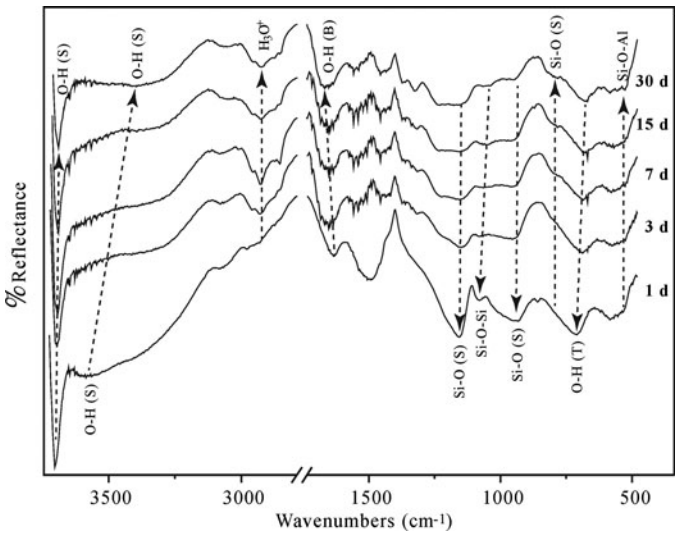

Fig. 5. FTIR spectra for the reacted mineral surfaces in the bioleaching experiment (28°C) from day 1 to day 30. The dotted line with an arrow denotes the major changes and shifts of the bonds.

et al. 2005; Lapeyrie et al. 1987). In our study, the fact that fungal cells produced more organic acids in the presence than in the absence of minerals (Table 3) was largely in line with these previous results because dissolution of lizardite released high concentrations of soluble metals and silica as buffering components into the system.

Here we note that high concentrations of Mg^{2+}/Ni^{+} have no recognizable benefits but adverse effects on fungal cells, but some other elements like Fe (~3.5% in lizardite) in serpentine were crucial in fungal cell growth and showed an influence over fungal production of organic acids. The difference in fungal metabolic activities (in the absence and presence of lizardite) might also be caused by the basic microenvironment at the lizardite surfaces, where more organic acids were necessary to protect the fungal growth of surface-bound hyphae.

Fungal Bioleaching-Efficiency and Mechanisms

The chosen fungal isolate showed great potential in bioleaching Mg^{2+} from lizardite. In this study, up to 40 wt.% of Mg^{2+} was released into solution at ambient conditions (28°C and 1 atm), ~ 80% higher than that reported by Daghino et al.

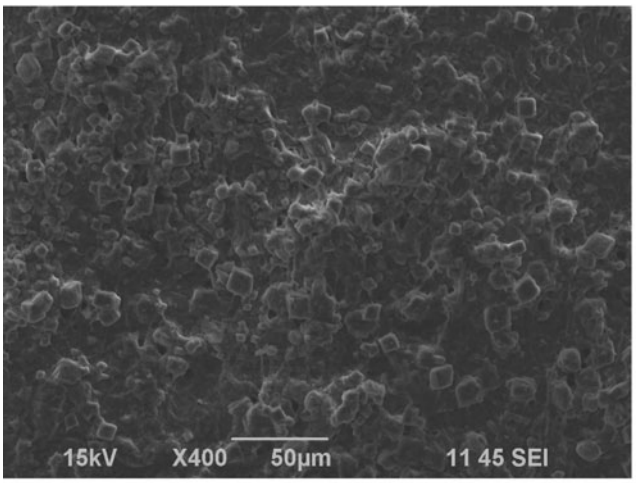

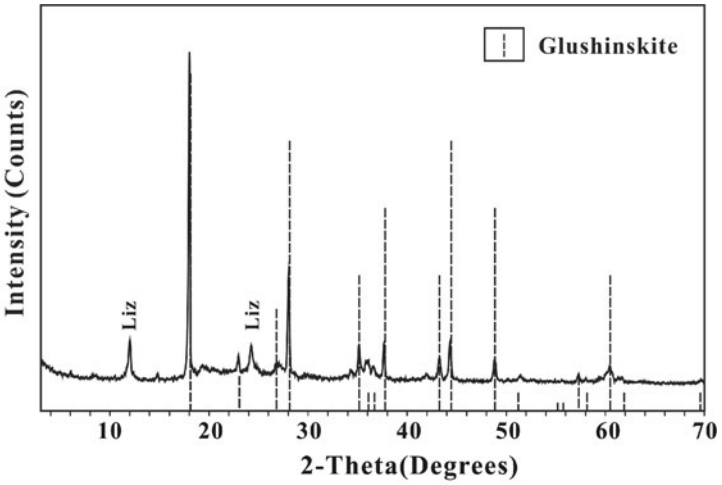

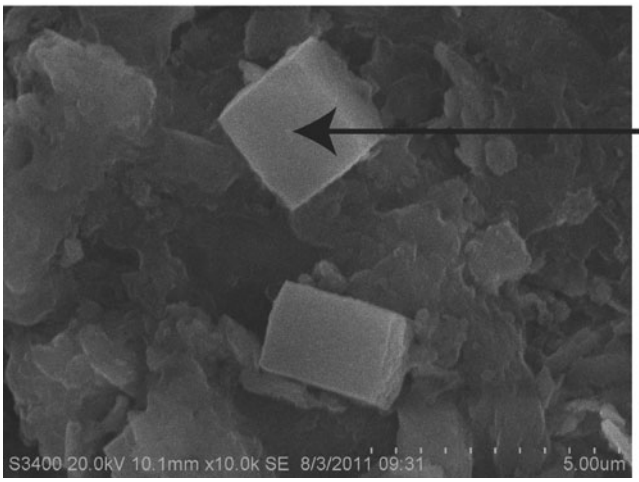

Element	Weight%	Atomic%
C K	36.03	45.24
O K	49.6	46.76
Na K	1.06	0.69
Mg K	6.48	4.02
Si K	3.55	1.9
K K	1.45	0.56

Fig. 6. SEM, EDS, and XRD analyses of the reacted lizardite at the end of the bioleaching experiments at 38°C, confirming the formation of secondary mineral glushinskite ($MgC_2O_4 \cdot 2H_2O$).

Table 4. Chemical analyses for the experimental solutions at day 1, 3, 7, 15, and 30 in 18, 28, and 38°C bioleaching systems, respectively

	18°C				28°C				38°C			
Time	pH	Glucose ($g \cdot L^{-1}$)	Mg (ppm)	Si (ppm)	pH	Glucose ($g \cdot L^{-1}$)	Mg (ppm)	Si (ppm)	pH	Glucose ($g\ L^{-1}$)	Mg (ppm)	Si (ppm)
1	5.50	19.96	0	0	5.50	19.96	0	0	5.50	19.96	0	0
3	5.73	18.81 ± 0.32	29.91 ± 1.75	19.90 ± 1.33	4.63	16.73 ± 0.35	105.13 ± 4.28	64.39 ± 1.21	5.25	15.74 ± 1.00	101.74 ± 7.99	51.13 ± 1.62
7	4.67	14.92 ± 0.14	63.64 ± 3.41	39.14 ± 4.71	4.96	9.12 ± 1.26	232.90 ± 15.56	96.60 ± 1.21	4.75	6.70 ± 1.24	407.27 ± 10.67	114.48 ± 6.00
15	4.22	6.64 ± 1.32	159.79 ± 8.79	62.05 ± 2.26	5.91	2.44 ± 1.35	418.48 ± 19.45	63.63 ± 1.11	5.81	1.18 ± 0.42	461.56 ± 21.02	76.22 ± 1.48
30	5.85	3.22 ± 1.36	244.34 ± 11.10	73.72 ± 2.36	6.13	0.630.26	441.33 ± 26.33	72.49 ± 0.71	5.96	0.15 ± 0.08	522.14 ± 36.87	67.38 ± 3.27

(2009) using *Verticillium leptobactrum*. We also estimated the dissolution rates of lizardite based on the temporal change of $[Mg^{2+}]$ in the solution (Table 4), and found that the rates ranged from 10^{-12} to 10^{-10} $mol \cdot m^{-2} \cdot s^{-1}$ in our experiments, ~3–4 orders of magnitude higher than those in abiotic systems in the literature (Benedetti et al. 1994; Freyssinet and Farah 2000; Pačes 1983; Tu et al. 2011).

The dissolution of lizardite in an acidic environment may be expressed by the following eq.:

$$Mg_3Si_2O_5(OH)_4 + 6H^+ \rightarrow 3Mg^{2+} + 2SiO_2 + 2H_2O \quad (2)$$

The protons in the bioleaching experiments were mainly derived from fungal production of organic acids, which also provided substantial amounts of ligands to the system. Previous studies (Drever and Stillings 1997; Furrer and Stumm 1986; Stumm 1997; Welch and Ullman 1996) proposed that in the presence of polyfunctional acids such as oxalate and succinate, the dissolution of silicate minerals was controlled by both proton- and ligand-promoted mechanisms. For example, in the case of plagioclase, poly-acids including oxalate, citrate, succinate, pyruvate, and 2-ketoglutarate, were found to be the most effective at promoting dissolution relative to mono-acids such as acetate although both types of organic acids were far more effective than inorganic acids (Welch and Ullman 1993).

The observation that the fungal system achieved far higher Mg release rates and efficiency (Figure 1) in comparison to the pH-adjusted (with HCl) fungus-free control in our experiments was consistent with this previous understanding. It was also suggested that the degree of ligand-promoted enhancement of dissolution rates would increase with decreasing acidity. In our study, the pH in the fungal experiments decreased quickly from 5.5 to ~4.5 in the first three days and rebounded quickly before finally reaching circum-neutral levels in the following days, likely due to the addition of dissolved silica (the pH of control B was also maintained accordingly).

Interestingly, we found that the dissolution rates in the inorganic (control B) and biotic (fungal) started to diverge around day 4 / day 5 when both solution pH was ~ 6, suggesting that the ligand-promoted dissolution accounted for a major part in the fungal bioleaching of lizardite. Another consideration regarding the difference between control B and fungal samples was the pKa values of the inorganic and organic acids. The major organic acids produced by fungi have relatively higher pKa's that HCl (with a pKa of -6). Specifically, the pKa was 1.23 and 4.19 for oxalic acid, 3.86 for gluconic acid, 3.03 and 4.44 for fumaric acid, and 3.75 for formic acid. Thus, at the same acidic pH, solutions containing organic acids had much higher buffering capacity than those containing inorganic strong acids (e.g., HCl), and this subtility was difficult to be incorporated into the controls.

Although the focus of this study was on the release efficiency of Mg^{2+}, Si concentrations in the solution were also monitored, and by comparing the concentration ratios of Mg versus Si, we obtained some information concerning the dissolution nature and mechanisms of lizardite. As shown in Figure 4, Mg-depleted, silica-rich layers were detected at the reacted mineral surfaces, which correlated well with the high [Mg]/[Si] ratios in the experimental solutions (Table 4/Figure 7).

As the thickness of the surface leached layer increased, the inner Mg-OH octahedral might become inaccessible to protons and/or ligands as well as fungal hyphal tips for direct

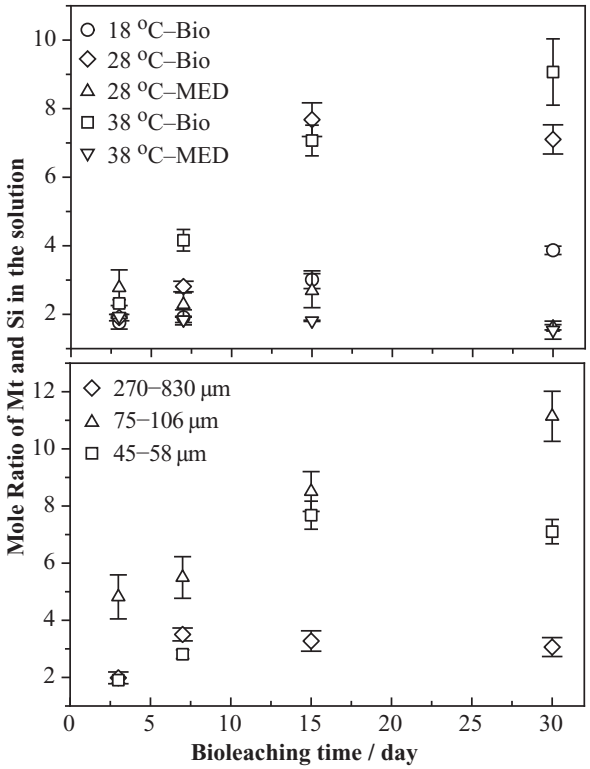

Fig. 7. Molar ratios of $[Mg^{2+}]$ versus $[Si^{4+}]$ in the experimental solution at 18, 28 and 38°C from the bioleaching system (top). The results for different particle sizes at 28°C were also presented (bottom).

interaction. Thus, the extent of Mg^{2+} release / equilibrium of lizardite dissolution was likely controlled by the properties of these surface silica layers (Madejova et al. 1998). The factors that influenced the solubility and structures of the amorphous silica layers, like temperature, pH, the presence of organic ligands, and physical forces, had probably affected the Mg-release rate and efficiency as well.

Mg-release efficiency in the fungal system depends on both temperature and particle sizes. In the range of 18°C–38°C, higher efficiency and dissolution rates were achieved with increased temperature, which may have affected the reaction equilibrium and kinetics (Equation 1) by elevating the system energy levels and/or by enhancing the fungal activities in terms of acid and ligand production. The solubility of amorphous silica was also higher when temperature rose from 18°C to 38°C. Therefore, the overall temperature effect on Mg release from lizardite was a result from a combination of factors including the enhanced proton and ligand concentrations, the accelerated kinetics, and the enhanced dissolution of surface silica layers.

The particle size, on the other hand, controlled the availability of mineral surface areas for reactions with aqueous species (Holdren Jr. and Berner 1979; Kump et al. 2000; Schott et al. 1981) and with fungal cells (hypha). The correlation of the initial and intermediate dissolution rates with the available mineral surface areas, however, seemed to be non-linear due to the incongruent nature of lizardite dissolution in the presence of fungi. This non-linear relationship also suggested that the surface structures of the original and reacted minerals were susceptible to direct fungus-mineral interactions. The assisting role of fungal hypha in accelerating mineral breakdown by penetrating into the bulk along boundaries, cleavages, and fractures was previously documented (Adeyemi and Gadd 2005).

Bonneville et al. (2009) found that biotite dissolution was first induced by biomechanical forcing of hypha and then by biochemical alteration at the fungus-biotite interface. Due to the specific size of fungal hypha (~5–10 μm in dia), the fungus-particle contact and interaction might be most effective on particles of a certain size range (neither too small nor too large). In our experiments, the highest [Mg]/[Si] ratio (~9 at day 30) was observed in the sample solution of medium-sized particles rather than the smallest-sized particles (~7 at day 30), indicating that other than providing protons and ligands, fungal cells might have participated in the bioleaching process by modifying the amorphous silica layer on the reacted mineral surfaces.

Conclusion

The isolated fungal strain showed remarkable tolerance to high concentrations of Mg^{2+} and Ni^{2+} and high efficiency (relative to abiotic process) of Mg extraction, implicating a good potential of this organism to solubilizing metals from serpentine rocks. A possible application of this finding is the bioleaching of Mg^{2+} for carbon sequestration via mineral carbonation. Not only can this strategy improve metal extraction efficiency, reduce material and energy cost associated with chemical extraction processes, it is also environmentally more friendly and advantageous for future green development.

Acknowledgments

We thank the anonymous reviewers for their critical and constructive comments.

Funding

Financial support for this study was provided by China Geological Survey (Grant No. 1212011087126), Natural Science Fund of Jiangsu Province (Grant No. BK2011017), and US DOE Basic Energy Science Program (Grant No. DE-FG02-02ER15366).

References

Adeyemi AO, Gadd GM. 2005. Fungal degradation of calcium-, lead- and silicon-bearing minerals. Biometals 18(3):269–281.

Banfield JF, Barker WW, Welch SA, Taunton A. 1999. Biological impact on mineral dissolution: Application of the lichen model to understanding mineral weathering in the rhizosphere. Proc Natl Acad Sci 96(7):3404–3411.

Béarat H, McKelvy MJ, Chizmeshya AVG, Sharma R, Carpenter RW. 2002. Magnesium hydroxide dehydroxylation/carbonation reaction processes: Implications for carbon dioxide mineral sequestration. J Am Ceram Soc 85(4):742–748.

Benedetti MF, Menard O, Noack Y, Carvalho A, Nahon D. 1994. Water-rock interactions in tropical catchments: field rates of weathering and biomass impact. Chem Geol 118(1–4):203–220.

Bonneville S, Smits MM, Brown A, Harrington J, Leake JR, Brydson R, Benning LG. 2009. Plant-driven fungal weathering: Early stages of mineral alteration at the nanometer scale. Geology 37(7):615–618.

Burford EP, Kierans M, Gadd GM. 2003a. Geomycology: fungi in mineral substrata. Mycologist 17(3): 98–107.

Burford EP, Fomina M, Gadd GM. 2003b. Fungal involvement in bioweathering and biotransformation of rocks and minerals. Mineral Mag 67(6): 1127–1155.

Castro IM, Fietto JLR, Vieira RX, Tropia MJM, Campos LMM, Paniago EB, Brandao RL. 2000. Bioleaching of zinc and nickel from silicates using Aspergillus niger cultures. Hydrometallurgy 57(1):39–49.

Daghino S, Martino E, Vurro E, Tomatis M, Girlanda M, Fubini B, Perotto S. 2008. Bioweathering of chrysotile by fungi isolated in ophiolitic sites. FEMS Microbiol Lett 285(2):242–249.

Daghino S, Turci F, Tomatis M, Girlanda M, Fubini B, Perotto S. 2009. Weathering of chrysotile asbestos by the serpentine rock-inhabiting fungus Verticillium leptobactrum. FEMS Microbiol Ecol 69(1):132–141.

Drever JI, Stillings LL. 1997. The role of organic acids in mineral weathering. Coll Surf A: Physicochem Eng Asp 120(1–3):167–181.

Dutton MV, Evans CS. 1996. Oxalate production by fungi: its role in pathogenicity and ecology in the soil environment. Can J Microbiol 42(9):881–895.

Favero-Longo SE, Girlanda M, Honegger R, Fubini B, Piervittori R. 2007. Interactions of sterile-cultured lichen-forming ascomycetes with asbestos fibres. Mycol Res 111: 473481.

Fomina M, Burford EP, Hillier S, Kierans M, Gadd GM. 2010. Rock-Building Fungi. Geomicrobiol J 27(6–7):624–629.

Fomina M, Hillier S, Charnock JM, Melville K, Alexander IJ, Gadd GM. 2005. Role of oxalic acid overexcretion in transformations of toxic

metal minerals by Beauveria caledonica. Appl Environ Microbiol 71(1):371–381.
Freyssinet P, Farah ASd. 2000. Geochemical mass balance and weathering rates of ultramafic schists in Amazonia. Chem Geol 170(1–4):133–151.
Furrer G, Stumm W. 1986. The coordination chemistry of weathering: I. Dissolution kinetics of δ-Al_2O_3 and BeO. Geochim Cosmochim Acta 50(9):1847–1860.
Gadd GM. 2007. Geomycology: biogeochemical transformations of rocks, minerals, metals and radionuclides by fungi, bioweathering and bioremediation. Mycol Res 111:3–49.
Gadd GM, Raven JA. 2010. Geomicrobiology of Eukaryotic Microorganisms. Geomicrobiol J 27(6–7):491–519.
Gardes M, Bruns TD. 1993. Its primers with enhanced specificity for Basidiomycetes - Application to the identification of Mycorrhizae and Rusts. Mol Ecol 2(2):113–118.
Gleeson D, Clipson N, Melville K, Gadd G, McDermott F. 2005. Characterization of fungal community structure on a weathered pegmatitic granite. Microb Ecol 50(3): 360–368.
Goff F, Lackner KS. 1998. Carbon dioxide sequestering using ultramafic rocks. Environ Geosci 5(3): 89–102.
Gorbushina AA. 2006. Fungal activities in subaerial rock-inhabiting microbial communities. In: Gadd GM, editor. Fungi in Biogeochemical Cycles. Cambridge, UK: Cambridge University Press. p267–288.
Gulis V, Kuehn K, Suberkropp K. 2006. The role of fungi in carbon and nitrogen cycles in freshwater ecosystems. In: Gadd GM, editor. Fungi in Biogeochemical Cycles. Cambridge, UK: Cambridge University Press. p404–435.
Herzog H. 2002. Carbon Sequestration via Mineral Carbonation: Overview and Assessment. MIT Laboratory for Energy and the Environment. Cambridge, MA: MIT.
Hoffland E, Kuyper TW, Wallander H, Plassard C, Gorbushina AA, Haselwandter K, Holmstrom S, Landeweert R, Lundstrom US, Rosling A, Sen R, Smits MM, van Hees PA, van Breemen N. 2004. The role of fungi in weathering. Front Ecol Environ 2(5):258–264.
Holdren Jr GR, Berner RA. 1979. Mechanism of feldspar weathering-I. Experimental studies. Geochim Cosmochim Acta 43(8):1161–1171.
Huijgen WJ, Witkamp G-J, Comans RN. 2005. Mineral CO_2 sequestration by steel slag carbonation. Environ. Sci. Technol. 39(24): 9676–9682.
Jackson TA, Keller WD. 1970. A comparative study of the role of lichens and" inorganic" processes in the chemical weathering of recent Hawaiian lava flows. Am J Sci 269(5):446–466.
Kloprogge JT, Frost RL, Rintoul L. 1999. Single crystal Raman microscopic study of the asbestos mineral chrysotile. Phys Chem Chem Phys 1(10):2559–2564.
Krevor SCM, Lackner KS. 2011. Enhancing serpentine dissolution kinetics for mineral carbon dioxide sequestration. Int J Greenh Gas Con 5(4):1073–1080.
Kump LR, Brantley SL, Arthur MA. 2000. Chemical, weathering, atmospheric CO_2, and climate. Annu Rev Earth Pl Sci 28:611–667.
Lackner KS, Wendt CH, Butt DP, Joyce EL, Sharp DH. 1995. Carbon-dioxide disposal in carbonate minerals. Energy 20(11):1153–1170.
Lapeyrie F, Chilvers GA, Bhem CA. 1987. Oxalic-acid synthesis by the mycorrhizal fungus *Pazillus Involutus* (Batsch ex Fr) Fr. New Phytol 106(1):139–146.
Madejova J, Bujdak J, Janek M, Komadel P. 1998. Comparative FT-IR study of structural modifications during acid treatment of dioctahedral smectites and hectorite. Spectrochim Acta A 54(10):1397–1406.
Pacala S, Socolow R. 2004. Stabilization wedges: Solving the climate problem for the next 50 years with current technologies. Science 305(5686):968–972.
Pačes T. 1983. Rate constants of dissolution derived from the measurements of mass balance in hydrological catchments. Geochim Cosmochim Acta 47(11):1855–1863.
Pal A, Ghosh S, Paul AK. 2006. Biosorption of cobalt by fungi from serpentine soil of Andaman. Bioresource Technol 97(10):1253–1258.
Palmer R, Siebert J, Hirsch P. 1991. Biomass and organic acids in sandstone of a weathering building: Production by bacterial and fungal isolates. Microb Ecol 21(1):253–266.
Post JL, Borer L. 2000. High-resolution infrared spectra, physical properties, and micromorphology of serpentines. Appl Clay Sci 16(1–2): 73–85.
Power IM, Dipple GM, Southam G. 2010. Bioleaching of Ultramafic Tailings by *Acidithiobacillus spp*. for CO_2 Sequestration. Environ. Sci. Technol 44(1):456–462.
Schott J, Berner RA, Sjöberg EL. 1981. Mechanism of pyroxene and amphibole weathering-I. Experimental studies of iron-free minerals. Geochim Cosmochim Acta 45(11):2123–2135.
Stolaroff JK, Lowry GV, Keith DW. 2005. Using CaO-and MgO-rich industrial waste streams for carbon sequestration. Energ Convers Manage 46(5):687–699.
Stumm W. 1997. Reactivity at the mineral-water interface: dissolution and inhibition. Coll Surf A: Physicochem Eng Asp 120(1–3):143–166.
Teir S, Kuusik R, Fogelhohn CJ, Zevenhoven R. 2007a. Production of magnesium carbonates from serpentinite for long-term storage of CO_2. Int J Miner Proc 85(1–3):1–15.
Teir S, Eloneva S, Fogelholm CJ, Zevenhoven R. 2009. Fixation of carbon dioxide by producing hydromagnesite from serpentinite. Appl Energ 86(2):214–218.
Teir S, Revitzer H, Eloneva S, Fogelholm CJ, Zevenhoven R. 2007b. Dissolution of natural serpentinite in mineral and organic acids. Int J Miner Proc 83(1–2):36–46.
Tu V, Baumeister J, Metcalf R, Olsen A, Hausrath E. 2011. Serpentine weathering and implications for Mars. 42nd Lunar and Planetary Science Conference, Woodlands, Texas 1608:2303.
Welch SA, Ullman WJ. 1993. The effect of organic acids on plagioclase dissolution rates and stoichiometry. Geochim Cosmochim Acta 57(12):2725–2736.
Welch SA, Ullman WJ. 1996. Feldspar dissolution in acidic and organic solutions: Compositional and pH dependence of dissolution rate. Geochim Cosmochim Acta 60(16):2939–2948.